Modelling the Output Process of an ATM Multiplexer with Correlated Priorities

N.L.S. Fonseca J.A. Silvester,

Relatório Técnico IC 96-12

Agosto de 1996

I) INTRODUCTION

The future Broadband Integrated Services Digital Network will carry video, voice and data applications with different Quality of Service requirements. The cell arrival stream from integrated traffic is highly correlated and neglecting its correlations leads to a dramatic underestimation of the delay and loss rate. The departure (output) process of an ATM multiplexer is also correlated. Only recently has attention been given to the analysis of the output process of ATM multiplexers [1]-[6]. However, just few works have considered networks with prioritized flows. In this paper, we introduce a procedure for modelling the output process of an ATM switching node [7]-[13] in which the priority level of the arriving cells are correlated. Moreover, we specify a framework for queueing networks with prioritized Markov modulated flows.

Only recently, have some studies derived the statistical properties of the output process of queues with Markov Modulated input [1]-[4]. Saito [1] studied the output process of the N/G/1 queue and particularly of the MMPP/D/1 queue. By comparing the z-transform curves of the covariance of interarrival times for both input and output processes of a queue, Saito concluded that covariances are likely to be preserved. Takine et al. [2] derived expressions for the k^{th} moment of the interdeparture time and the statistics of busy and idle periods of a queue with Discrete-time Batch Markovian Arrival Process input (D-BMAP/D/1/K queue). Park et al. [3] proposed a procedure for matching the output process of a 2-MMBP/Geo/1/K queue with the statistics of a two state Markov Modulated Bernoulli Process (2-MMBP). The statistics used were: mean and variance of interdeparture time, the autocorrelation of the interdeparture time and of the counting process with lag one. Fonseca and Silvester [4] modelled the output process of a D-BMAP/D/1/K queue as a two-state Markov Modulated Bernoulli Process. They matched the long-term index of dispersion for counts and covariances at lags one and two. This procedure is reasonably accurate. Percentage errors of the delay and of the loss rate estimation were respectively under 6.5% and 10%. This procedure was extended to consider ATM multiplexer with selective discard mechanism in which the priority level of a cell is independent of other cells. Percentage errors of the high and of the low priority classes were respectively under 15% and 10%. The priority independence assumption is quite reasonable as a first order approximation. However, a more detailed analysis is need in order to capture the existing bursts of high/low priority cells which corresponds to conformance/violation periods of a rate control mechanism. In the present work, we show how to model the output process of an ATM multiplexer with correlated priority flow.

The precise estimation of end-to-end performances depends on the accurate representation of the flows in the network. To completely specify a queueing network framework, we need to define three network flow operations: output process, splitting and joining [14]-[15]. In [16], we illustrated how a framework for queueing networks with Markov modulated flows can be used to compute end-to-end delays in ATM networks. Our results were quite encouraging. We found percentage errors under 9% in a twenty nodes tandem network and under 7% in networks with feed-forward topology. In order to analyze ATM networks, we extend our framework to include flows with correlated priority.

This paper is organized as follows. Section II describes a framework for queueing networks with Markov modulated flows. In section III we introduce a model for the output process of a prioritized multiplexer. In section IV, we show numerical examples and finally some conclusions are drawn in section V.

II) A QUEUEING NETWORK FRAMEWORK WITH PRIORITIZED MARKOV MODULATED FLOWS

We assume that the input traffic of the queueing network is modelled as a prioritized Discrete Time Batch Markovian Arrival Process (D-BMAP$^{[H,L]}$). A D-BMAP $^{[H,\ L]}$ is a D-BMAP process where arrivals can be classified as either high or low priority. In the Discrete Time Batch Markovian Arrival Process [17]-[19], a batch may arrive at every discrete time. The batch size probability mass function depends on the state of an underlying Markov chain. A D-BMAP is completely specified by the matrices D_n whose elements $(d_{ij})_n$ give the probability that a transition from state i to state j occurs and a batch of size

n arrives. In a D-BMAP $^{[H, L]}$ the probability of an arrival (cell) belong to a certain priority class (priority probability) depends on the priority of the previous cell in the flow. After a period with no-arrivals, the priority probability of the first arriving cell is independent of any other cell in the flow. Thus, the "memory" of the priority classification exists between two no-arrival periods. Let us define $\theta = (p_{H/NO}, p_{H/H,}, p_{L/L})$ where:

$p_{H|NO}$ - is the probability that the first cell after a period with no arrivals be high priority

$p_{H|H}$ - is the probability of a cell being high priority given that the previous one was also high priority;

$p_{L|L}$ - is the probability of a cell being low priority given that the previous one was also low priority;

We define a correlation measure ψ as $p_{H|H} + p_{L|L}$ - 1. If $p_{H|NO} = p_{H|H} = 1 - p_{L|L}$ (and consequently $\psi = 0$) we have independent priorities. A positive value of ψ indicates that cells of at least one of the classes tend to be agglutinated in bursts, meanwhile a negative value of ψ shows that for at least one class there is no tendency of burst formation. The maximum value of ψ (=1) happens when $p_{H|H} = p_{L|L} = 1$ and corresponds to the situation in which we have whole bursts of just one priority level.

We consider open queueing networks. In each node there is a single server with constant service time. The buffer space is organized as complete sharing with push-out. The drop policy is Last-In-First-Drop and service is provided in a First-Come-First-Served basis. In order to solve this queueing network with non-renewal flows, we employ the parametric decomposition approximation [14]-[15]. The parametric decomposition approximation evaluates the queues in the network as if they were stochastically independent. The queues are analyzed in isolation only after the input flow parameters are computed.

To complete specify a queueing network framework we need to define the stochastic process resulting from: i) departures of a queue (output process), ii) splitting of a process due to routing and iii) merging of processes which go to the same queue (joining). We define the network flow operators as:

Output process

At each discrete time, there is at most one single departure from the queue. In addition, the output process of a queue with Markov modulated process is correlated. Thus, we represent the output process as a prioritized Markov Modulated Bernoulli Process. We focus our attention on the two-state representation due to its low computational complexity. The 2-MMBP$^{[H, L]}$ is totally specified by θ, and by $\phi = (p_1, p_2, \alpha_1, \alpha_2)$ where p_i (i =1,2) is the probability of having an arrival when the underlying Markov chain is in state i, and α_i (i=1,2) is the transition probability in state i at each time instant. In the next section, we specify a procedure to represent the output process as a 2-MMBP$^{[H,L]}$.

Splitting

We assume that routing is memoryless which means that the probability of a cell departing from one node and going to another node is fixed. When characterizing the flow between two nodes, we represent the output process of the first queue as an MMBP$^{[H,L]}$ process with parameters $\phi = (p_1, p_2, \alpha_1, \alpha_2)$ and $\theta = (p_{H|NO}, p_{H|H}, p_{L|L})$, and then we model the flow that goes to the target queue as a second MMBP$^{[H,L]}$ with parameters $\tilde{\phi} = (p_{ij} \times p_1, p_{ij} \times p_2, \alpha_1, \alpha_2)$ and $\tilde{\theta} = (\tilde{p}_{H|NO}, \tilde{p}_{H|H}, \tilde{p}_{L|L})$ where:

p_{ij} - is the probability that a cell leaves node i and goes to node j,

$\tilde{p}_{H|H} = p_{H|H};$

$\tilde{p}_{L|L} = p_{L|L};$

$\tilde{p}_{H|NO} = p_{H/NO} \times p_0 + p_{high} \times (1 - p_0);$

$$p_0 = (1-p_1)\frac{\alpha_2}{2-\alpha_1-\alpha_2} + (1-p_2)\frac{\alpha_1}{2-\alpha_1-\alpha_2}$$ - is the probability of having no output process cell generation

$$p_{high} = \frac{1-p_{L|L}}{2-p_{H|H}-p_{L|L}}$$ - is the unconditional probability of a cell from the output process be high priority

Note that it is implicit in $\tilde{p}_{H|H}$ (and in $\tilde{p}_{L|L}$) that two consecutive cells of the output process are forward to the target destination. Regarding $\tilde{p}_{H|NO}$ we need to consider that the absence of cells in the target destination can be either due to the absence of cells in the output process or due to the forwarding of a cell to a different destination.

Alternate splitting operators such as correlated splitting [20] can be developed beyond memoryless splitting.

Joining

The superposition of two D-BMAP processes, *A* and *B*, with m_a, m_b states and n_a, n_b maximum batch size is also a D-BMAP, process *C*, with $m_c = m_a \, x \, m_b$ states and $n_c = n_a + n_b$ maximum batch size. The matrix $D_k^{(c)}$ with elements $(d_{ij})_k$ specifies the probability of going from state *i* to state *j* and having a batch arrival of size *k* and is computed as:

$$D_k^{(c)} = \sum_{q=0}^{min\lceil n_1, k\rceil} D_q^{(a)} \otimes D_{k-q}^{(b)}$$

where $A \otimes B$ denotes the Krockener product of matrix *A* by matrix *B*.

To compute the aggregate process priority probability, $\theta^{(c)}$ we need to take into consideration not only the priority probability of each aggregating process but also their probability of arrivals. Thus, we have:

$$p_{H|H}^{(c)} = \sum_{n_a=0}^{N_a} \sum_{n_b=0}^{N_b} \frac{n_i - n_j}{n_i + n_j} \times p_{H|H}^{(j)} + \frac{2n_j}{n_i + n_j} \times p_{high}^{(i)} p_{high}^{(j)} \times p_{n_a}^{(a)} \times p_{n_b}^{(b)} \quad n_a + n_b > 0$$

$$p_{H|NO}^{(c)} = p_{H|NO}^{(a)} \times \frac{1 - p_0^{(a)}}{\left(1 - p_0^{(a)}\right) + \left(1 - p_0^{(b)}\right)} + p_{H|NO}^{(b)} \times \frac{1 - p_0^{(b)}}{\left(1 - p_0^{(a)}\right) + \left(1 - p_0^{(b)}\right)}$$

where:

$$(i,j) = \begin{cases} (a,b) & n_a \geq n_b \\ (b,a) & n_a < n_b \end{cases}$$

$p_{n_i}^{(i)}$ - is the probability of having n_i arrivals from process i ($i=a,b$)

$p_{high}^{(i)}$ - is the unconditional probability of having a high priority arrival in process i

The $p_{L|L}^{(c)}$ expression is similar to the $p_{H|H}^{(c)}$ except for the index “high” which is replaced by the index “low” and for the index “H|H” which is replaced by the index “L|L”

III)THE OUTPUT PROCESS OF A D-BMAP$^{[H,L]}$/D/1/K QUEUE

In a work-conserving queue, a cell is lost if and only if it finds the buffer space full. Consequently, if we disregard the priority classification of the cells, we notice that the statistics of the output process of a D-BMAP$^{[H,L]}$/D/1/K is the same of the output process of a D-BMAP/D/1/K. Therefore, we compute the parameters for the output process in two steps. In the first step, we model the output process as a two state MMBP without taking into account the priority classification (we compute $\hat{\phi} = (\hat{p}_1, \hat{p}_2, \hat{\alpha}_1, \hat{\alpha}_2)$). In the second step, we compute $\hat{\theta} = (\hat{p}_{H|NO}, \hat{p}_{H|H}, \hat{p}_{L|L})$ (Figure 1).

The First Step

The output process of a queue with Markov modulated inputs is a correlated single arrival process. If we define the underlying Markov chain state as being the number of cells in the system plus the state of the input process, we are able to exactly represent the output process as a Markov Modulated Bernoulli Process. For instance, If we have a gated server (i.e., if a cell finds the server empty at its arrival slot, it can only be transmitted at the next slot) then, the matrices $\hat{D}_0$ and $\hat{D}_1$ are given by [17]:

$$\hat{D}_0 = \begin{bmatrix} D_0 & D_1 & \dots & D_{k-1} & \sum_{n=k}^{\infty} D_n \\ 0 & 0 & \dots & 0 & 0 \\ \dots & \dots & \dots & \dots & \dots \\ 0 & 0 & \dots & 0 & 0 \end{bmatrix}$$

$$\hat{D}_1 = \begin{bmatrix} 0 & 0 & 0 & \dots & 0 & 0 \\ D_0 & D_1 & D_2 & \dots & D_{k-1} & \sum_{n=k}^{\infty} D_n \\ 0 & D_0 & D_1 & \dots & D_{k-2} & \sum_{n=k-1}^{\infty} D_n \\ \dots & \dots & \dots & \dots & \dots & \dots \\ 0 & 0 & 0 & \dots & D_0 & \sum_{n=1}^{\infty} D_n \end{bmatrix}$$

Unfortunately, the exact MMBP representation is computationally unfeasible given that the number of states to represent the process at the output of each queue grows as a function of the buffer size and the number of states of the input process. Thus, we approximately represent the output process as a two-state MMBP. We do so by matching some statistics of the output process with the same statistics of the two-state MMBP. We chose to use the long-term index of dispersion for counts (the mean to the variance ratio) and the covariance of the count process at lags one and two.

We showed that these mentioned statistics result in accurate modelling of the output process [4]. The matching procedure was extensively validated. The percentage error of the delay and of the loss rate estimation were respectively under 7% and 10% in a two node tandem network when the output process of the first queue is replaced by a two-state MMBP [4]. We have used the matching procedure to estimate the end-to-end delay in tandem and in feed-forward networks [16]. End-to-end performance results were within a similar range of the percentage error for isolated queues. In an experiment with a 20 node tandem network, the end-to-end delay error was less than 2% higher than the error when we considered an isolated multiplexer. We have also used different D-BMAP to validate the matching procedure and found similar results for different processes [21].

__The Second Step__

Given that we have already characterized the aggregate output process, we need to compute the conditional probabilities that a cell belongs to a certain priority class. If we had an infinite buffer space the output priority probability, $\hat{\theta}$, would be the same as the input process priority probability, θ. However, in a finite buffer queue, we need to take into account the loss rate per class due to buffer overflow. We compute $\hat{\theta}$ by equating the unconditional (high/low) priority probabilities of the output process and of its D-BMAP$^{[H,L]}$ representation. Moreover, we approximate the (priority/loss) probability by the (priority/loss) rate. Thus, we have:

$$\hat{p}_{H|NO} = p_{H|NO}$$

$$\frac{1-\hat{p}_{H|H}}{2-\hat{p}_{H|H}-\hat{p}_{L|L}} = \frac{\left(1-p_{H|H}\right)\times(1-R_{low})}{\left(1-p_{L|L}\right)\times(1-R_{high})+\left(1-p_{H|H}\right)\times(1-R_{low})}$$

$$\frac{1-\hat{p}_{L|L}}{2-\hat{p}_{H|H}-\hat{p}_{L|L}} = \frac{\left(1-p_{L|L}\right)\times(1-R_{high})}{\left(1-p_{L|L}\right)\times(1-R_{high})+\left(1-p_{H|H}\right)\times(1-R_{low})}$$

where:

R_{high} - high priority loss rate

R_{low} - low priority loss rate

In order to compute the loss rate in a D-BMAP$^{[H,L]}$/D/1/K queue, we use a loss rate conservation law [24]. This law allows a solution with low computational complexity. The conservation law establishes that the product of the aggregated loss rate by the aggregated arrival rate is equal to summation of the per class product of the loss rate by the arrival rate. In other words:

$$\lambda R = \sum_{n=1}^{N} \lambda_n R_n$$

where λ and R are respectively the aggregated arrival rate and aggregated loss rate and λ_n and R_n are respectively the class n arrival rate and loss rate. The loss rate law is a generalization of Clare and Rubin's loss probability law for *i.i.d.* arrivals [22], and Jeon and Viniotis' law for Markov Modulated Poisson Processes.

To solve the D-BMAP$^{[H,L]}$/D/1/K queue, we first solve the aggregated system by computing the queue length distribution. We then derive the low priority loss rate by observing a tagged low priority cell and computing the probability that it is not dropped (successfully transmitted) [7].

A detailed solution of the D-BMAP$^{[H,L]}$/D/1/K queue, as well as a proof of the conservation law can be found in [24].

V) NUMERICAL EXAMPLES

In this section we discuss the main findings regarding the accuracy of the computational procedure. Extensive validation data can be found in [24]. We also show a tandem network example.

To verify the precision of our model, we consider two queues in tandem. The input of the first queue is a D-BMAP$^{[H, L]}$ and the input of the second queue is the result of the superposition of an interfering D-BMAP$^{[H, L]}$ and the output process of the first queue. The interfering process is introduced in order to avoid the "non-queueing" phenomenon in tandem networks. We compare the estimated loss rate per class at the second queue when the output process is replaced by a two-state MMBP$^{[H, L]}$ (Figure 2) with loss rate given by a simulation experiment. We report the percentage error which is defined as $\left|\frac{p_{sim} - p_{est}}{p_{sim}}\right| \times 100$ where p_{sim} is the probability given by the simulation experiment and p_{est} is the loss rate computed when we use the matching procedure. In the simulation experiments, we use independent replication method with 95% confidence interval. To avoid any distortion of the percentage error, we limit the range of simulation results to those which can be obtained through Monte Carlo techniques (from 10^{-8} to 10^{-1}); therefore avoiding the use of rare event simulation [25].

The input to the first queue and the interfering process are both two state D-BMAP$^{[H, L]}$ with the same transition probability in each state (α) [2]. The batch size is Poisson distributed with mean $(1 + c)\,\rho$ (state 1) and $(1 - c)\,\rho$ (state 2) where ρ is the overall traffic intensity and c is a parameter. It was demonstrated in [2] that the square coefficient of variation (C_v^2) and the correlation coefficient of the number of arrivals at lag n ($C_c(n)$) are respectively given by:

$$C_v^2 = \rho^{-1} + c^2$$

$$C_c(n) = \frac{c^2\rho}{1 + c^2\rho} \times (2\alpha - 1)^n$$

We consider that the probability that a cell belongs to a priority class does not depend on the state of the underlying Markov chain for both input and interfering processes.

Tables 1 and 2 show respectively the high and the low priority loss rate for a wide range of values. Our procedure is more accurate when it estimates loss rate for the low priority class than it is for the high priority class. The errors of the low priority loss rate estimation are similar to the errors of the aggregated loss rate. We also notice that our procedure is more precise for high values of the loss rate than it is for lower ones. Errors were below 17% for the high priority class and below 13% for the low priority class.

In order to evaluate the impact of the offered load, its coefficient of variation and its correlation coefficient on the accuracy of the procedure, we vary respectively ρ,c and α. Figure 3 show the high priority loss rate as a function of ρ (for input $\phi = (c = 0.9, \alpha = 0.9)$ $\theta = (0.9, 0.8, 0.5)$ and interfering $\phi = (\rho = 0.4, c = 0.5, \alpha = 0.9)$ and $\theta = (0.9, 0.8, 0.5)$). In the top part of the figure, we show the actual analytical and the simulation values and in the bottom part we show the corresponding percentage error. As the offered load increases, our procedure becomes more accurate. Figure 4 shows the percentage error as a function of ρ for different values of $p_{H|H}$. We note that the procedure is more precise for higher values of $p_{H|H}$ (for longer high priority bursts). Figure 5 and 6 are respectively similar to figure 3 and 4 except that it is for the low priority class. The same remark of Figure 3 applies to Figure 5. We note that for the low priority class the impact of the priority burst length is less significant than it is for the high priority class.

Figure 7 and 8 respectively display the percentage error of the high and of the low priority class when we vary c (for input $\phi = (\rho = 0.8, \alpha = 0.9), \theta = (0.9, 0.8, 0.5)$ and interfering $(\rho = 0.4, c = 0.1, \alpha = 0.9), \theta = (0.9, 0.8, 0.5))$. We notice that our procedure gives slightly more accurate results for higher values of the input process coefficient of variation. The impact of the coefficient of variation on the precision is a little more pronounced for the high priority class than for the low priority one. For the high priority class the maximum difference in the percentage error is 3% whereas for the low priority class the maximum difference is 2%. For the high priority class, the accuracy increases significantly as $p_{H|H}$ increases. For the low priority class, the impact on the accuracy is much less significant when we increase $p_{L|L.}$ In our validation experiments we also noticed that the precision of the procedure as a function of the coefficient of variance depends on the correlation coefficient. For positively correlated streams, we found out that the procedure is approximately 2% more precise than for negatively correlated streams. Figure 9 and 10 show respectively the accuracy of the procedure as a function of the input process correlation coefficient for the high and for the low priority class. In other words, the procedure is slightly more accurate for positively correlated streams than for negatively correlated ones.

To make sure that the interfering process parameters did not impact our results, we varied the interfering process ρ, c and α. No significant impact on the precision of our results was found.

In Figure 11 we show an example of a four node tandem network where we vary the offered load to the first queue. The interfering process parameters is the same for the three other queues (the first queue does not have an interfering process) We compute the end-to-end loss rate as $1 - \Pi\ (1 - p_i)$ where p_i is the loss rate at queue i. In the top part of Figure 11 we show the end-to-end loss rate computed using the computational procedure and the simulation estimation. The bottom part of the figure shows the respective percentage error. We note that the precision increases as the offered load increases. Additional examples can be found in [24].

VI) CONCLUSIONS

In this paper, we introduce a procedure for modelling the output process of a D-BMAP$^{[H,L]}$/D/1/K queue with push-out buffer policing in which the priority level of a cell depends on the priority level of other cells in the flow. The modelling is carried out in two major steps. In the first step, we characterize the output process disregarding the priority mechanism. In the second phase, we compute the probability that a cell belongs to a priority class. Our procedure is shown to be accurate. Errors of the estimated high and low priority are respectively under 13% and 17%. Moreover, we describe a framework for the analysis of queueing networks with prioritized Markov modulated flow. We are currently validating the queueing network framework for more generally connected networks. We are also comparing the impact of different work-conserving buffer organizations on the end-to-ed loss rate.

VII) REFERENCES

[1]H. Saito, “The departure process of an N/G/1 Queue”, *Perfor. Eval*., 11, pp. 241-251, 1990.

[2]T. Takine, T. Suda and T. Hasegawa, “Cell loss and output process analyses of finite buffer discrete time queueing system with correlated arrivals”, in *Proc. of IEEE INFOCOM*, pp 1259-1268, 1993

[3]D. Park, H. G. Perros and H. Yamashita, “Approximate analysis of discrete-time tandem queueing networks with bursty and correlated input traffic and customers” to appear in Operation Research Letters.

[4]N. L. S. Fonseca and J. A. Silvester, “Modelling the output process of an ATM multiplexer with Markov modulated arrivals”, in *Proc of IEEE ICC’94*, pp. 721-725, 1994.

[5]J.F. Ren, J. W. Mark and J. W. Wong, “End-to-end performance in ATM networks”, *Proc of IEEE ICC’94*, pp. 996-1002, 1994.

[6]V. Frost and Q. Wang, “Estimation of cell loss probabilities for tandem ATM queues”, *Proc of IEEE ICC’94*, pp. 1019-1024.

[7]N. L. S. Fonseca and J. A. Silvester, “Estimating the loss probability in a multiplexer loaded with multi-priority MMPP streams”, in *Proc. IEEE ICC’93*, pp. 1037-1041, 1993.

[8]A. Y-M Lin and J. A. Silvester, “Priority queueing strategies and buffer allocation protocols for traffic control at an ATM integrated broadband switching system, *IEEE J. Select. Areas Commun.*, vol. 9, pp. 1524-1536, Dec. 1991

[9] Y. Le Boudec, “An efficient solution method for markov models of ATM links with loss priorities”, *IEEE J. Select. Areas Commun.*, vol. 9, pp. 408-417, Apr. 1991.

[10]H. Kroner, “Comparative performance study of space priority mechanisms for ATM networks”, in *Proc. IEEE INFOCOM’90*, pp. 1136-1143, 1990.

[11]J. Garcia and Olga Casals, “Stochastic models of space priority mechanisms with Markovian arrival processes”, Annals of Operation Research 35, pp. 271-296, 1992

[12]D. W. Petr and V. S. Frost, “Priority cell discarding for overload control in BIDN/ATM networks: an analysis framework”, International Journal of Digital and Analog Communication Systems, vol 3, n 2, 1990.

[13] N. L. S. Fonseca and J. A. Silvester, “A comparison of push-out policies in an ATM multiplexer”, in *Proc. of IEEE Pac. Rim Conf. on Commun. Comp. and Signal Proc*., pp. 338-341, 1993.

[14]P. J. Kuehn, “Approximate analysis of general queueing networks by decomposition”, *IEEE Trans. Commun*., vol COM-27, 1, pp. 113-126, 1979

[15] W. Whitt, “The Queueing Network Analyzer”, *The Bell Sys. Tech.l J*., vol. 62, pp. 2779-2815, Nov. 1983

[16]N. L. S. Fonseca and J. A. Silvester, “ On the computation of end-to-end delay in feed-forward ATM networks”, *Proc. of IEEE International Telecommunication Symposium’94,* pp. 460-464.

[17]C. Blondia, “A discrete-time batch Markovian arrival process as B-ISDN traffic model”, *Belgian J. of Oper Res., Stat. and Comp. Science*, vol. 32 (3), pp. 3-23, 1992.

[18] S. Wang and J. A. Silvester, “A discrete-time performance model for integrated service ATM multiplexers”, in *Proc. of IEEE GLOBECOM’93,* pp.757-761, 1993

[19] C. Blondia and O. Casals, “Performance analysis of a statistical multiplexing of VBR sources”, *Proc of IEEE INFOCOM*, pp 828-838, 1992

[20]I. Stavrakakis, “Efficient modeling of merging and spliting processes in large networking structures”, *IEEE J. Select. Areas Commun*., vol 9, no 8, pp. 1336-1347, Oct. 1991.

[21]J. A. Silvester, N. L. S. Fonseca and S.S. Wang, “D-BMAP models for the perfor-

mance evaluation of ATM networks", in Proc of 2nd IFIP Workshop on Performance and Modeling of ATM networks", paper n^{o} 34, 1994.

[22]L. P. Clare and I. Rubin, "Performance boundaries for prioritized multiplexing systems", *IEEE Trans on Info. Theory*, n^{o} 3, pp. 329-340, May 1987.

[23]Y-H Jeon and I. Viniotis,"Achievable loss probabilities and buffer allocation policies in ATM nodes with correlated arrivals", in *Proc of IEEE ICC'93*, pp. 352-358, 1993

[24] N. L. S. Fonseca , "Queueing Network Models for Multiple Class Broadband Integrated Services Digital Networks", U.S.C. CENG Tech Report 94-25, 1994

[25]M. Devetsikiotis and J.K. Townsend, "Statistical Optimization of Dynamic Important Sampling Parameters for Efficient Simulation of Communication Networks", IEEE/ACM Transactions on Networking, pp 293-305, vol 1 n 3, June 1993.

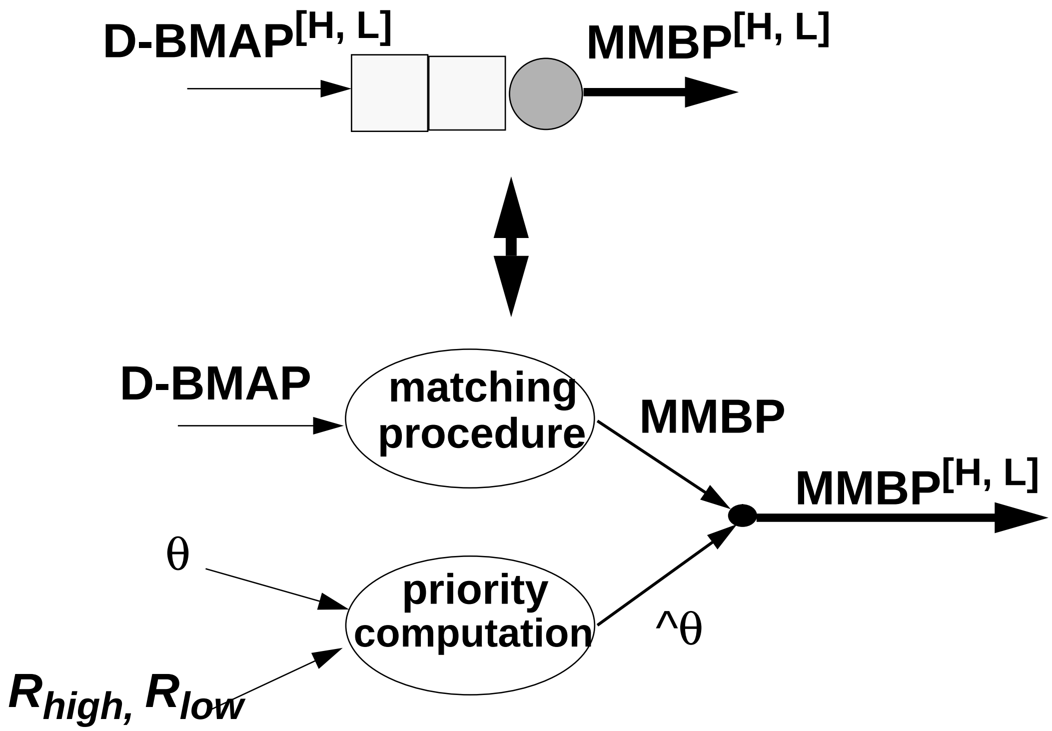

Figure 1: The computational procedure for the modelling of an ATM multiplexer with selective discard.

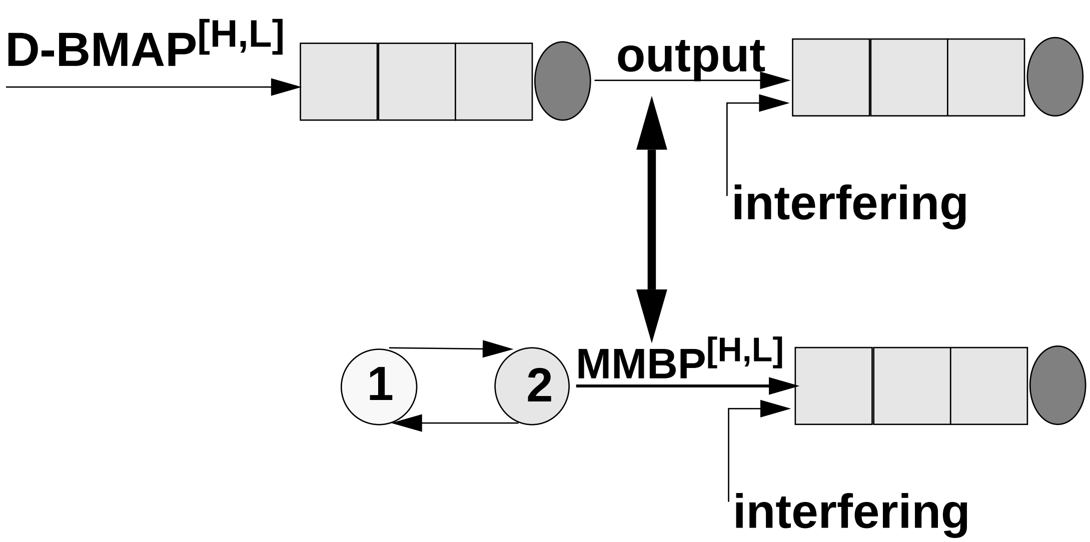

Figure 2: Scheme for validation of the matching procedure.

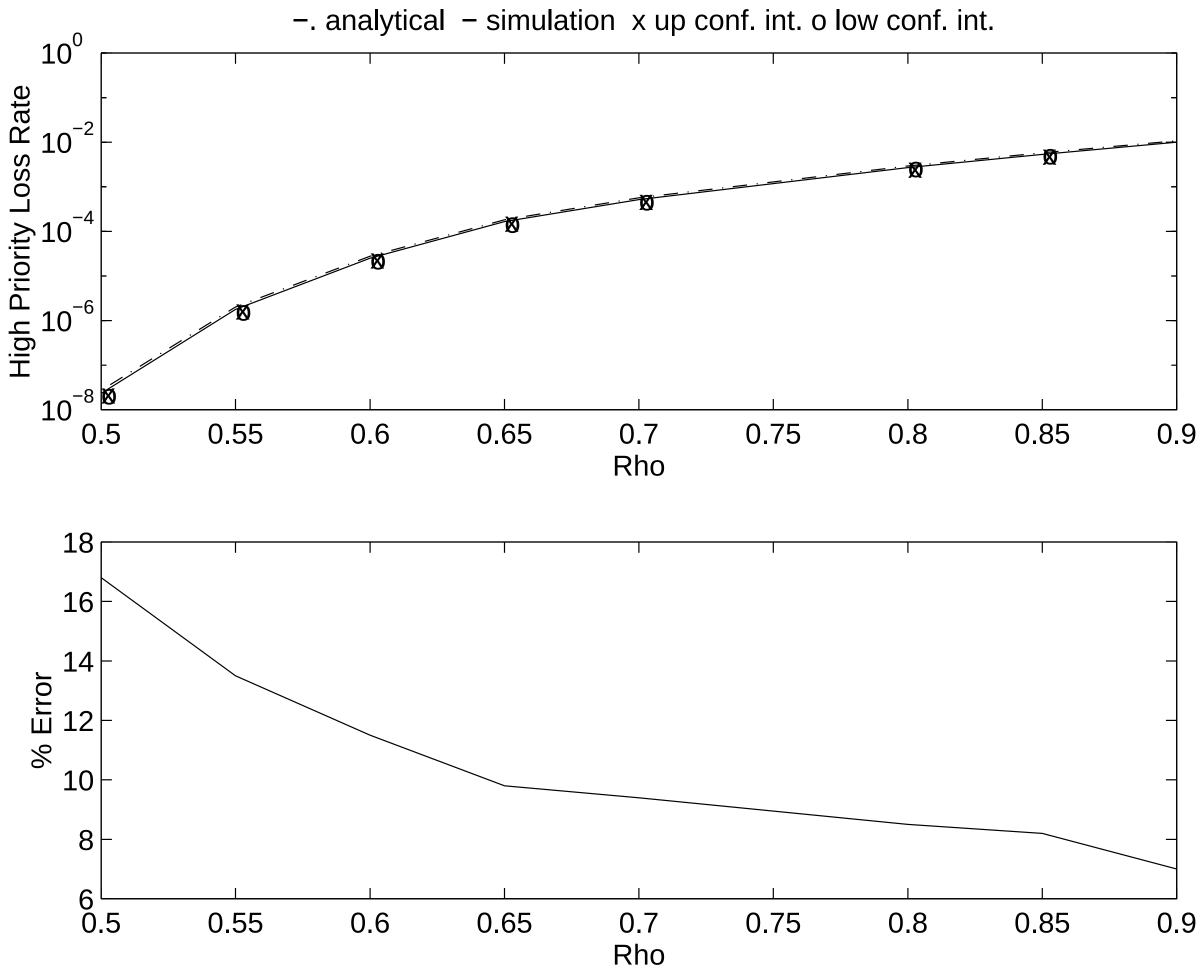

Figure 3: High priority Loss rate x offered load

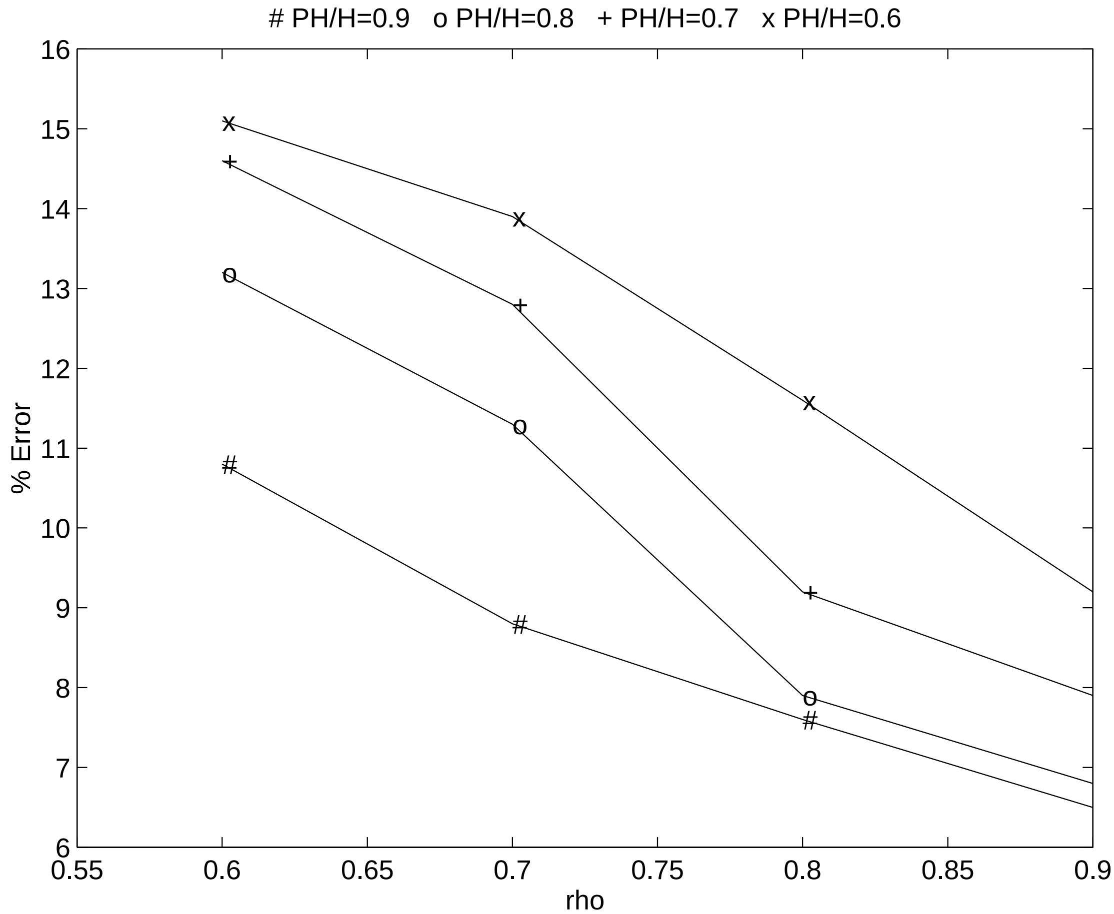

Figure 4: Percentage error of the high priority loss rate x offered load

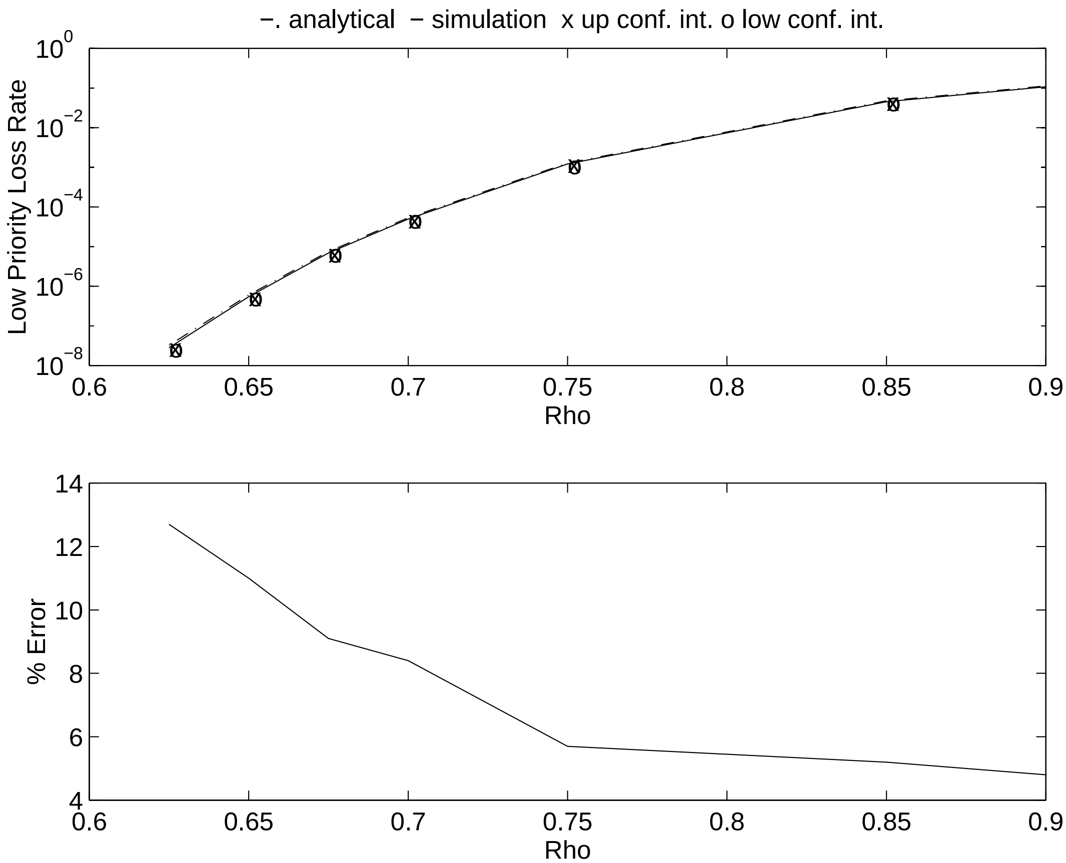

Figure 5: Low priority loss rate x offered load

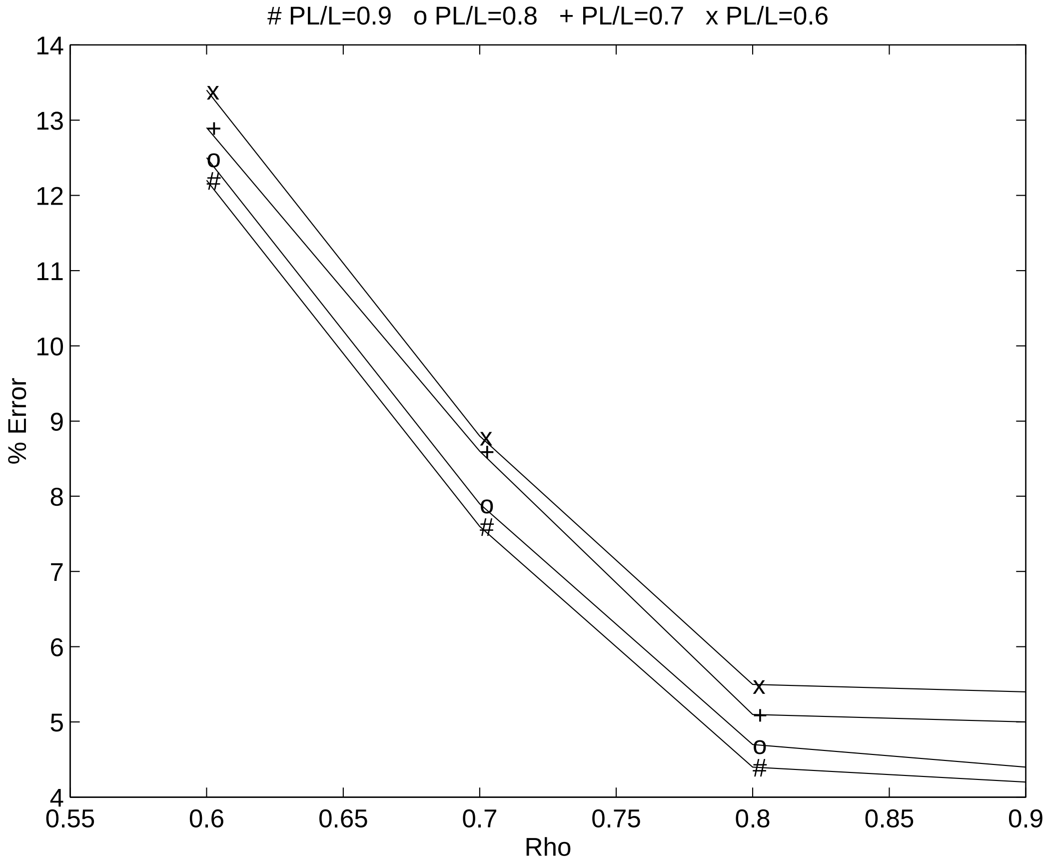

Figure 6: Low priority loss rate x offered load

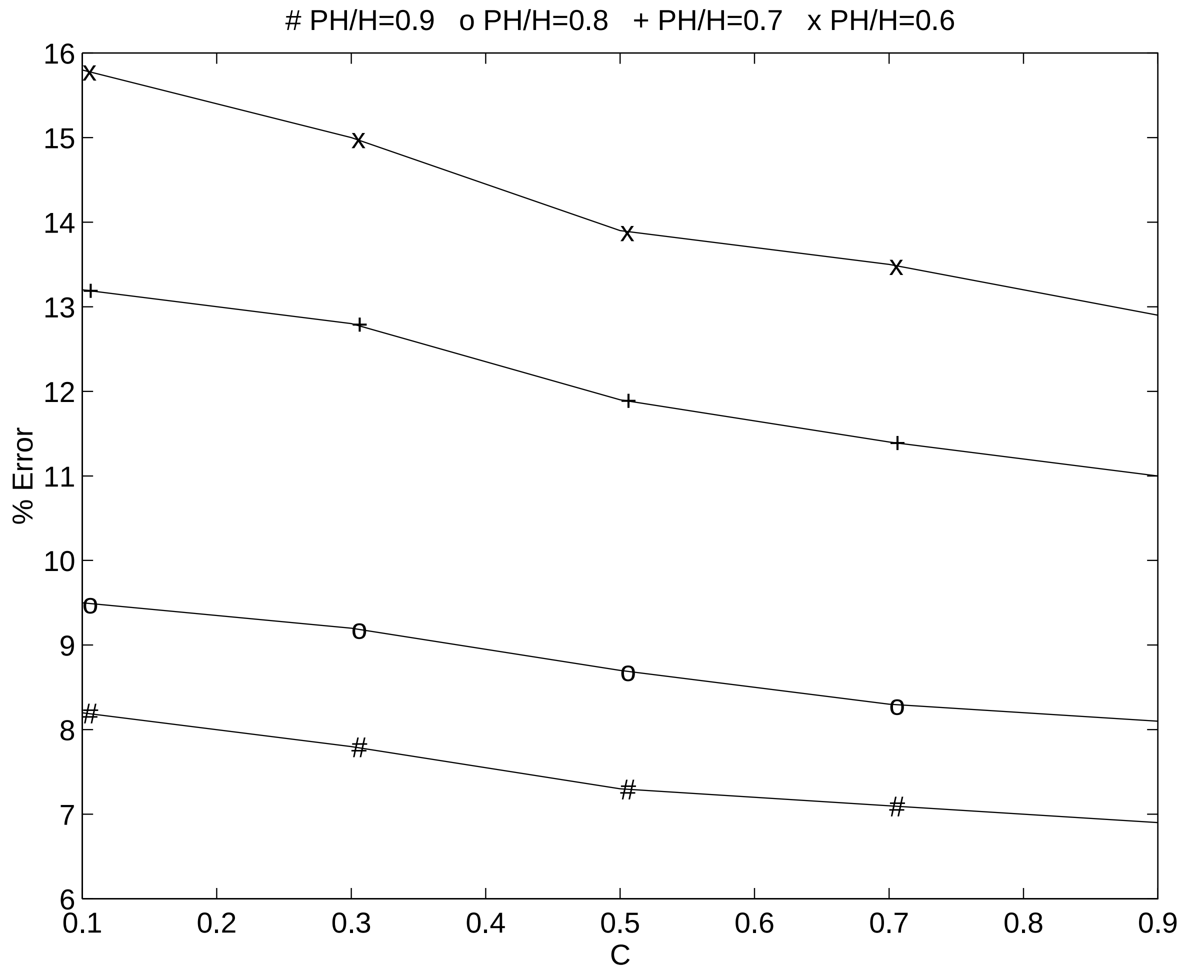

Figure 7: Percentage error of the High priority class loss rate x c

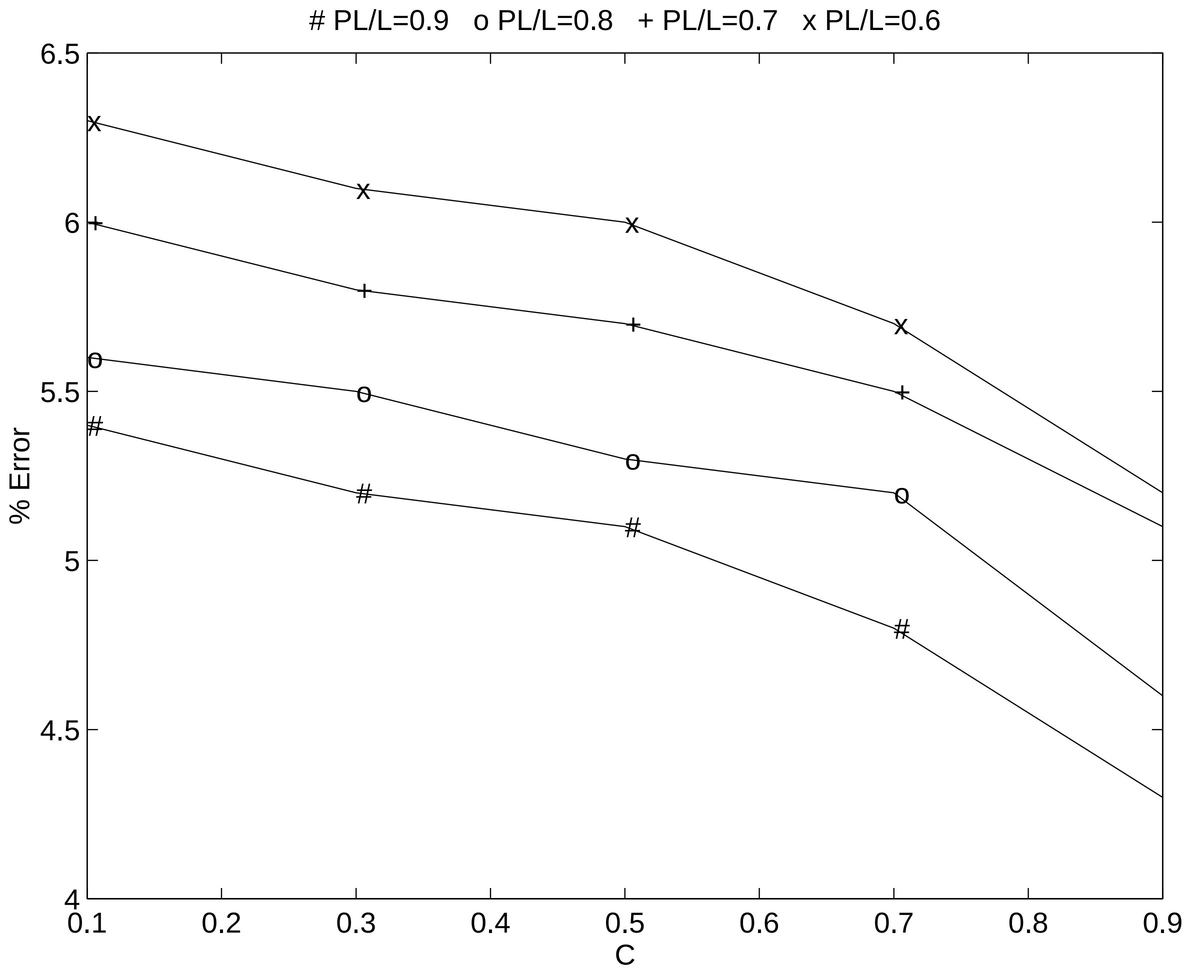

Figure 8: Percentage error of the low priority class loss rate x c

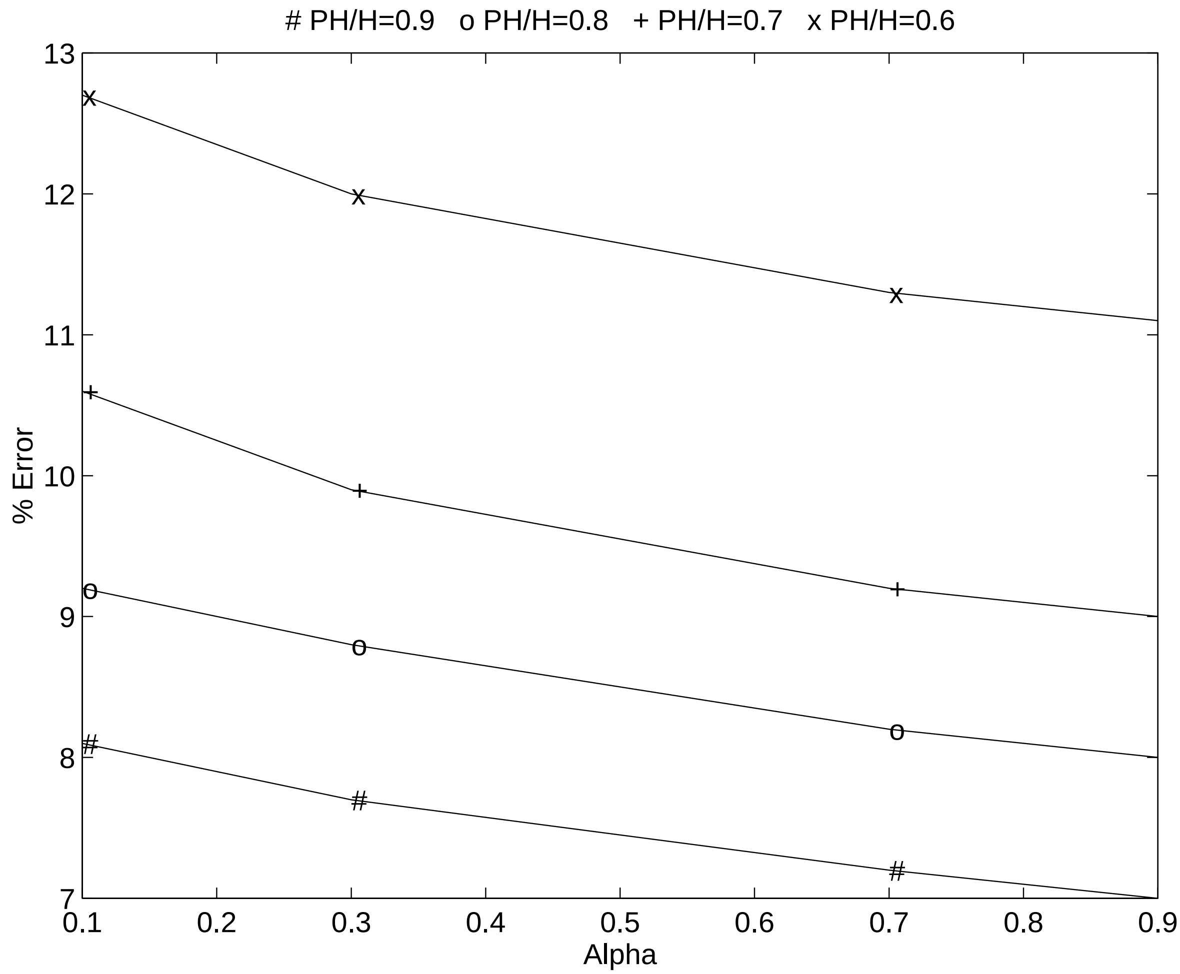

Figure 9: Percentage error of the High priority class loss rate x α

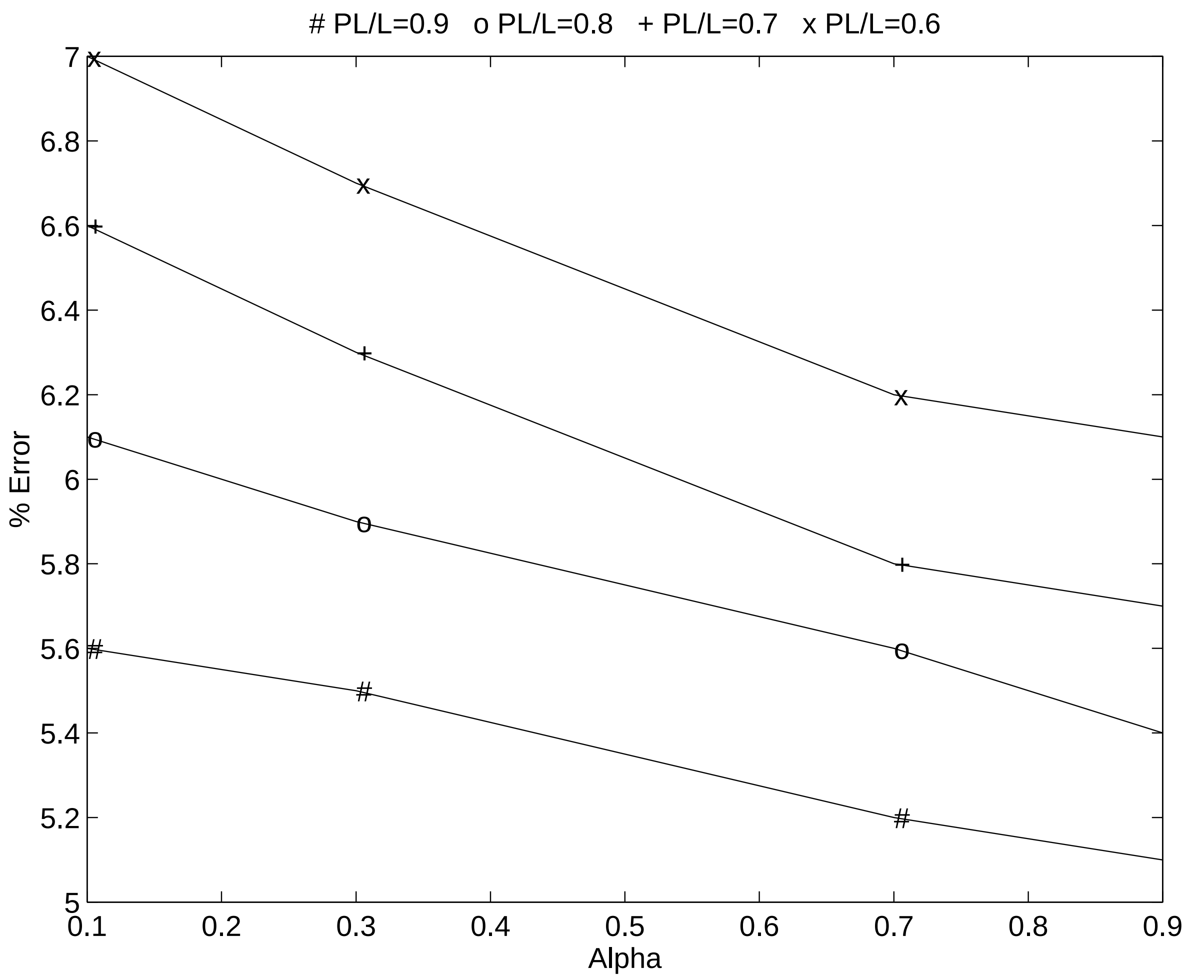

Figure 10: Percentage error of the low priority class loss rate x α

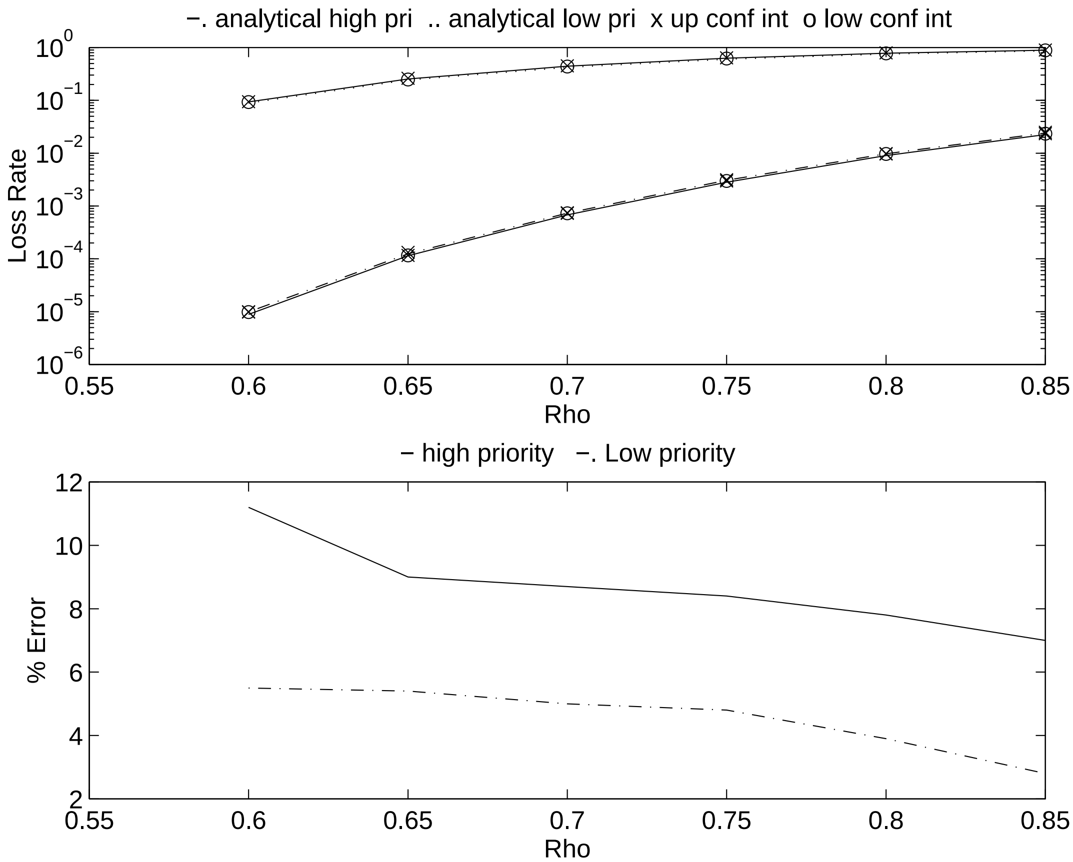

Figure 11: A tandem network example